Progress In Electromagnetics Research, PIER 26, 223–248, 2000

ON THE EFFECT OF ATMOSPHERIC EMISSION UPON THE PASSIVE MICROWAVE POLARIMETRIC RESPONSE OF AN AZIMUTHALLY ANISOTROPIC SEA SURFACE

N. Pierdicca

University "La Sapienza" of Rome
Department of Electronic Engineering
via Eudossiana 18-00184 Rome, Italy

F. S. Marzano

University of L'Aquila
Department of Electrical Engineering
67040 Poggio di Roio, L'Aquila, Italy

L. Guerriero

University of Tor Vergata
Department of Informatics, Systems and Production
via di Tor Vergata-00133 Rome, Italy

Paolo Pampaloni

C.N.R.-I.R.O.E.
Via Panciatichi 64-50127 Florence, Italy

1. INTRODUCTION

The retrieval of near-surface ocean wind on a global scale is of relevant interest for many oceanographic applications and for the study of ocean-atmosphere interactions. On one hand, the near-surface wind produces the momentum flux affecting the ocean circulation and, on the other hand, it represents a key driving force in the air-sea exchange processes [1]. Spaceborne and airborne microwave scatterometers have been extensively used to estimate near-surface wind fields [2]. In the last decade satellite-based microwave radiometry has proved to be a potential tool for ocean wind remote sensing due to the fact that microwave thermal emission from sea surfaces is affected by surface roughness and thus indirectly by wind motion at various scales, and also by temperature, foam, salinity and the state of the atmosphere between the sensor and the target surface [3]. In particular, ocean surface wind speed estimations have been successfully performed by using the polarization diversity of the Special Sensor Microwave Imager (SSM/I) aboard the Defense Meteorological Space Program (DMSP) near-polar orbiting platforms [4]. Moreover, synergic inversion for active and passive microwave remote sensing of the ocean surface characteristics have been also proposed and carried out [5, 6].

Although it is commonly accepted that microwave radiometers can retrieve ocean wind speed based on the sensivity of thermal emission to surface roughness, only in the last years it has been shown that microwave radiometric measurements are sensitive to wind direction too [7]. Airborne campaigns and analyses of SSM/I measurements have indicated that ocean brightness temperatures can vary over azimuthal angles relative to the wind direction by a few degrees Kelvin [7–10]. These experimental evidences have been supported by theoretical studies about the sensitivity of the polarimetric passive signature, that is

the observed Stokes vector, over an azimuthally-anisotropic surface [11–13]. Polarimetric emission from the ocean surface has been modelled with various approximations, from the simplified one-dimensional periodic case to the more realistic random two- dimensional model based on the small perturbation approach [14, 15]. A remarkable result of these theoretical studies is that the third Stokes vector (which expresses basically the correlation between the horizontal and the vertical components of the electric field) is mainly sensitive to the azimuthal angle between the wind direction and the looking angle, the root-mean-square height of the surface and to the surface wave-height spectrum.

Spaceborne passive polarimeters for ocean remote sensing, having channels in the K and K_a band (between 15 and 40 GHz), have recently been proposed [16]. Airborne polarimetric radiometers have been designed and used for experimental activities at 14.3 GHz, at 19.3 GHz and 91.6 GHz [17, 9, 10]. For frequencies higher than 10 GHz the atmospheric effects due to e.m. extinction and scattering cannot be neglected, especially when in presence of clouds and rain [18]. In order to properly investigate the sensitivity of passive polarimetric response to the ocean wind field, the impact of atmospheric emission on the measured Stokes vector has to be quantified. The simulation of the apparent brightness temperature vector at the platform height has to include both the upwelling and downwelling atmospheric radiation together with the bistatic scattering of downwelling brightness temperatures due to the rough sea surface as done in [9] and in the more recent paper by Yeong et al. [32]. To some extent, even the atmospheric stability in the boundary layer can have an impact on the polarimetric passive measurements [19].

In this work, we analyse the effect of the atmospheric emission on the polarimetric brightness temperature vector observed at the top-of-the-atmosphere due to an azimuthally-asymmetric wind-roughened ocean surface. In addition to what is done in [9] and [31], the latter is modeled through a two-scale and two-dimensional model in order to account for the geometrical tilting of the capillary waves due the underlying large scale gravity waves. The small-scale ocean scattering is described through a small perturbation model (SPM) to solve the scattering field up to the second order. The depolarising and isotropic effect of the foam coverage is also considered as a function of the wind speed, the frequency and the observation angle. An unpolarized radiative

transfer model (RTM) is used for taking into account a weakly scattering atmosphere, that is with presence of non-precipitating clouds and low to moderate rainfall. Supposing to use radiometric channels at 18.7 and 37.0 GHz , a statistical evaluation of the atmospheric contribution impact is carried out by using both radiosounding measurements and numerical outputs of a microphysical mesoscale cloud model. Finally, a simplified model function of the atmospheric effects on passive polarimetric response of the ocean wind fields is proposed as a possible premise to a statistical inversion scheme based on passive polarimetric measurements in clear and cloudy conditions.

2. THEORETICAL FORMULATION

After introducing the basic relationships, we will illustrate the atmospheric radiation transfer model utilized in this work and its coupling with the sea surface. Figure 1 shows the geometry of the problem, including the rough sea surface and the directions of incidence, scattering as well emission of the microwave radiation.

In this section we will refer to a very general sea surface roughness whose scattering will be described by the bistatic scattering coefficients. When performing numerical simulations in the subsequent sections, we will adopt a two-scale formulation. The bistatic scattering coefficients of capillary sea waves will be given by the Small Perturbation Model (SPM) and an incoherent summation of brightness temperatures from tilted rough patches will be required in order to account for the large waves.

2.1 Basic Relations in Radiopolarimetry

The relations between the modified Stokes vector $\mathbf{F_m}$ (Watt m^{-2} cycle^{-1} sec), the modified specific intensity $\mathbf{I_m}$ (Watt m^{-2} sterad^{-1} Hz^{-1}) and the vector of brightness temperature $\mathbf{T_B}$(K) that we use in this paper are the following:

$$\mathbf{F_m} = \begin{bmatrix} I_h \\ I_\nu \\ U \\ V \end{bmatrix} = \begin{bmatrix} \langle E_h E_h^* \rangle \\ \langle E_\nu E_\nu^* \rangle \\ 2\mathrm{Re}\langle E_\nu E_h^* \rangle \\ 2\mathrm{Im}\langle E_\nu E_h^* \rangle \end{bmatrix} = \frac{\eta d\Omega}{2\pi} \mathbf{I_m}$$

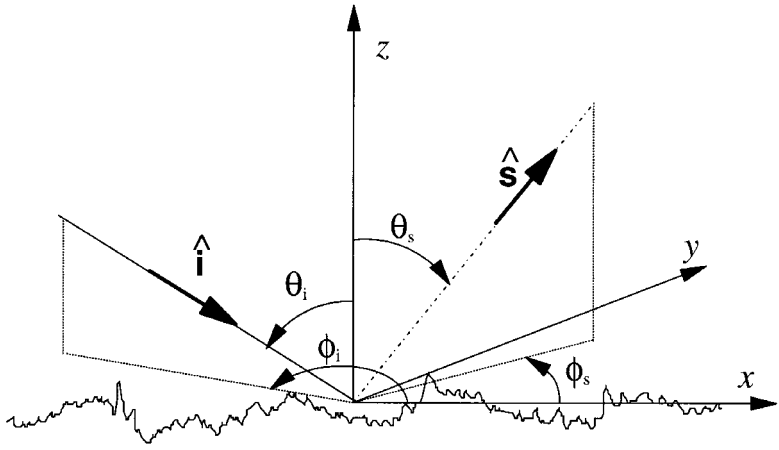

Figure 1. Geometry of the surface scattering problem.

$$= \frac{k2\eta d\Omega}{2\pi\lambda^2}\mathbf{T_B} = C\mathbf{T_B} = C\begin{bmatrix} T_{Bh} \\ T_{B\nu} \\ U/C \\ V/C \end{bmatrix} \tag{1}$$

where η is the intrinsic impedance of the media, k is the Boltzmann constant. Factor 2π accounts for the transformation of power per unit of angular frequency ω into power per unit of frequency, as required by the formulation of Yueh and Kwok [20].

The modified Mueller matrix linearly relates the modified Stokes vector of a plane wave illuminating an object from direction $\hat{\mathbf{i}}$ (ϑ_i, φ_i) to the Stokes vector of the scattered wave propagating in the direction $\hat{\mathbf{s}}$ (ϑ_s, φ_s) and observed at distance r from the object:

$$\mathbf{F}^s_{\mathbf{m}} = \frac{1}{r^2}\mathbf{M}(\hat{\mathbf{s}}, \hat{\mathbf{i}})\mathbf{F}^i_{\mathbf{m}} \tag{2}$$

$\hat{\mathbf{i}}$ and $\hat{\mathbf{s}}$ are unitary vectors while ϑ and φ are polar coordinates in a FSA (Forward Scattering Alignment) reference system [21].

If we consider an element of a rough surface of area A which is observed from direction $\hat{\mathbf{s}}$ at distance r and we assume that an angular spectrum of statistically independent plane waves is illuminating this portion of the surface, it is preferable to deal with the modified specific intensity vectors $\mathbf{I_m}$ or the brightness temperature vector $\mathbf{T_B}$ instead

of $\mathbf{F_m}$. By considering the radiation impinging upon the area A from an element of solid angle $d\Omega_i$ around direction $\hat{\mathbf{i}}$, for the radiation observed at direction $\hat{\mathbf{s}}$ we can derive the following equation:

$$\mathbf{I}^s_{\mathbf{m}} = \frac{2k}{\lambda^2}\mathbf{T}^s_{\mathbf{B}} = \frac{1}{A\cos\vartheta_s}\mathbf{M}(\hat{\mathbf{s}},\hat{\mathbf{i}})\mathbf{I}^i_{\mathbf{m}}d\Omega_i = \frac{2k}{\lambda^2 A\cos\vartheta_s}\mathbf{M}(\hat{\mathbf{s}},\hat{\mathbf{i}})\mathbf{T}^i_{\mathbf{B}}d\Omega_i \quad (3)$$

being the solid angle $d\Omega_s$ from which the area is observed given by $r^2 d\Omega_s = A\cos\vartheta_s$.

2.2 Unpolarized Radiative Transfer Model for Atmospheric Emission and Transmission

Assuming that the radiation emitted by the atmosphere is unpolarized, the solution of the radiative transfer equation for the brightness temperature $T_B(r)$ at distance r from the origin $r = 0$ of an optical path throughout the atmosphere is given by the following [2]:

$$\begin{aligned} T_B(r) = {} & T_B(0)e^{-\tau(0,r)} \\ & + \int_0^r k_e(r')[(1-w)T(r') + wT_{sc}(r')]e^{-\tau(r',r)}dr' \end{aligned} \quad (4)$$

where $T_B(0)$ is the incident brightness temperature at $r = 0$, T is the physical temperature and T_{sc} is the scattering source function; $k_e = k_a + k_s$ is the extinction coefficient at each point $r = r'$ of the optical path, being k_a and k_s the absorption and scattering coefficients, respectively; $w = w(r')$ is the single scattering albedo equal to k_s/k_e; $\tau(r', r)$ is the optical thickness from the generic source point to the observation point and $\tau(0, r)$ is the optical thickness of the entire optical path (i.e., the opacity). The transmittance of the atmosphere from r' to r is related to the optical thickness by the following:

$$\gamma(r', r) = e^{-\tau(r',r)} = e^{-\int_{r'}^{r} k_e(r'')dr''} \quad (5)$$

Equation (4) can be simplified if we assume that the atmosphere is plane-parallel, that is the atmospheric physical parameters depend only on the altitude z and they are independent on the horizontal co-ordinates x and y. Moreover, we can assume the atmospheric scattering is moderate enough to neglect the scattering source function (i.e., $Tsc = 0$). This implies either the absence of, or a very low atmospheric precipitation.

In this case, the atmosphere brightness temperature emitted downward with an incidence angle ϑ at the Earth surface $(z = 0)$ becomes:

$$T_{DN}(\pi - \vartheta; 0) = \sec\vartheta \int_0^\infty [1 - w(z')] k_e(z') T(z') e^{-\tau(0,z')\sec\vartheta} dz' \quad (6)$$

where $\sec(\vartheta) = 1/\cos(\vartheta)$. The integral extends from 0 to infinity but the function to be integrated is negligible above a given altitude (say 30 km). Therefore, the brightness temperature incident upon the Earth surface is given by:

$$\begin{aligned} T_B^i(\pi - \vartheta; 0) &= T_{COS} e^{-\tau(0,\infty)\sec\vartheta} + T_{DN}(\pi - \vartheta, 0) \\ &= T_{COS}\gamma_\vartheta(0,\infty) + T_{mDN}[1 - \gamma_\vartheta(0,\infty)] \end{aligned} \quad (7)$$

where T_{COS} is the cosmic background radiation (it is assumed unpolarized and equal to 2.7 K), $\tau(0,\infty)$ is the atmospheric opacity at zenith, $\gamma_\vartheta(0,\infty)$ is the transmittance of the atmosphere for a slant path and T_{mDN} is the downwelling mean radiative temperature defined as $T_{DN}(\pi - \vartheta, 0)/[1 - \gamma_\vartheta(0,\infty)]$. In a very similar way we can derive a relation for the upwelling brightness temperature emitted by a plane-parallel atmosphere in the ϑ direction and observed by a radiometer placed at altitude $z = H$:

$$\begin{aligned} T_{UP}(\vartheta; H) &= \sec\vartheta \int_0^H [1 - w(z')] k_e(z') T(z') e^{-\tau(z',H)\sec\vartheta} dz' \\ &= T_{mUP}[1 - \gamma_\vartheta(0, H)] \end{aligned} \quad (8)$$

The mean radiative temperatures T_{mDN} and T_{mUP} and the opacity τ completely describe the radiative behavior of the atmosphere. These quantities are related to the entire vertical profiles of the atmospheric temperature and composition in such a way to make it possible to replace the stratified atmosphere with an equivalent homogeneous layer. When considering the entire atmosphere, the atmospheric opacity is equal in both equations, while the radiative mean temperatures T_{mDN} and T_{mUP} for ground-based and space-based observations are generally different. It is interesting to note that the radiative temperatures can be known with fairly good accuracy since it can be related to the meteorological parameters of the atmosphere at the surface or even derived from climatological values related to the time of the year and to the geographical location.

For unpolarized atmospheric emission we can easily extend all the above considerations to the polarimetric notation. Analytically, the Stokes vector of the radiation incident upon the Earth surface at an angle ϑ with respect to nadir is given by the following:

$$\begin{aligned}\mathbf{F}^i_{\mathbf{m}}(\pi-\vartheta;0) &= \begin{bmatrix} I_h \\ I_\nu \\ U \\ V \end{bmatrix} = CT^i_B(\pi-\vartheta;0)\begin{bmatrix} 1 \\ 1 \\ 0 \\ 0 \end{bmatrix} \\ &= C\begin{bmatrix} T_{COS}\gamma_\vartheta(0,\infty)+T_{mDN}[1-\gamma_\vartheta(0,\infty)] \\ T_{COS}\gamma_\vartheta(0,\infty)+T_{mDN}[1-\gamma_\vartheta(0,\infty)] \\ 0 \\ 0 \end{bmatrix} \end{aligned} \quad (9)$$

The brightness temperature vector $\mathbf{T}^{TOA}_{\mathbf{B}}(\vartheta,\varphi;H)$ observed by a radiometer placed at an altitude H (Top Of the Atmosphere: TOA) is given by the unpolarized upward atmospheric emission plus the brightness temperature vector radiated by the surface $\mathbf{T}^{BOA}_{\mathbf{B}}(\vartheta,0)$ (Bottom Of the Atmosphere: TOA) multiplied by the transmission matrix of the atmosphere $\boldsymbol{\gamma}$. If we assume that the atmospheric scattering, when present, is due to spherical particles, $\boldsymbol{\gamma}$ is a diagonal matrix with element all equal to $\gamma_\vartheta(0,\infty)$ and we can write the following [22]:

$$\begin{aligned}&\mathbf{T}^{TOA}_{\mathbf{B}}(\vartheta,\varphi;H) \\ &\quad= \mathbf{T}^{BOA}_{\mathbf{B}}(\vartheta,\varphi;0)\boldsymbol{\gamma}+\mathbf{T}_{\mathbf{B}UP} \\ &\quad= \mathbf{T}^{BOA}_{\mathbf{B}}(\vartheta,\varphi;0)\begin{bmatrix} \gamma_\vartheta(0,H) & 0 & 0 & 0 \\ 0 & \gamma_\vartheta(0,H) & 0 & 0 \\ 0 & 0 & \gamma_\vartheta(0,H) & 0 \\ 0 & 0 & 0 & \gamma_\vartheta(0,H) \end{bmatrix} \\ &\qquad+\begin{bmatrix} T_{UP}(\vartheta;H) \\ T_{UP}(\vartheta;H) \\ 0 \\ 0 \end{bmatrix}\end{aligned} \quad (10)$$

The brightness temperature vector $\mathbf{T}^{BOA}_{\mathbf{B}}(\vartheta,\varphi;0)$ radiated by the Earth surface is composed by two contributions, the thermal emission $\mathbf{T}^{e}_{\mathbf{B}}$ of the surface and the downward atmospheric radiation scattered by the surface $\mathbf{T}^{s}_{\mathbf{B}}$. Both contributions are partially polarized if the surface roughness is not isotropic in azimuth and we will analyze in detail the latter component in the next paragraph.

2.3 Surface Scattering of Downwelling Atmospheric Radiation

Let us consider a rough sea surface in the absence of foam. If a partially coherent radiation impinges upon the Earth surface from direction $\vartheta_i,\ \varphi_i$ around the solid angle $d\Omega_i$ the modified specific intensity $\mathbf{I}_m^s$ of the radiation scattered in the direction $\vartheta_s,\ \varphi_s$ by a portion of the surface of area A is given by equation (4) (see Figure 1). The modified Mueller matrix $\mathbf{M}(\vartheta_s, \varphi_s; \vartheta_i, \varphi_i)$ is related to the scattering matrix $\mathbf{S}$ with elements $f_{\alpha,\beta}$ by the following equation [22]:

$$\mathbf{M}(\vartheta_s, \varphi_s; \vartheta_i, \varphi_i) = \begin{bmatrix} |f_{hh}|^2 & |f_{h\nu}|^2 & \mathrm{Re}(f_{hh}^* f_{h\nu}) & -\mathrm{Im}(f_{hh}^* f_{h\nu}) \\ |f_{\nu h}|^2 & |f_{\nu\nu}|^2 & \mathrm{Re}(f_{\nu h}^* f_{\nu\nu}) & -\mathrm{Im}(f_{\nu h}^* f_{\nu\nu}) \\ 2\mathrm{Re}(f_{\nu h} f_{hh}^*) & 2\mathrm{Re}(f_{\nu\nu} f_{h\nu}^*) & \mathrm{Re}(f_{\nu\nu} f_{hh}^* + f_{h\nu} f_{h\nu}^*) & -\mathrm{Im}(f_{\nu\nu} f_{hh}^* - f_{\nu h} f_{h\nu}^*) \\ 2\mathrm{Im}(f_{\nu h} f_{hh}^*) & 2\mathrm{Im}(f_{\nu\nu} f_{h\nu}^*) & \mathrm{Im}(f_{\nu\nu} f_{hh}^* + f_{\nu h} f_{h\nu}^*) & \mathrm{Re}(f_{\nu\nu} f_{hh}^* - f_{\nu h} f_{h\nu}^*) \end{bmatrix} \tag{11}$$

where subscripts α and β indicate either horizontal (h) or vertical (ν) polarizations. Moreover, the elements $f_{\alpha\beta}$ of the scattering matrix and the bistatic scattering coefficients $\gamma_{\alpha\beta\mu\nu}$ are also related by the following:

$$\gamma_{\alpha\beta\mu\nu}(\hat{\mathbf{s}}, \hat{\mathbf{i}}) = 4\pi \frac{f_{\alpha\beta} f_{\mu\nu}}{A \cos\vartheta_s} \tag{12}$$

By substituting equation (9) into equation (3) and by integrating over all the incident directions belonging to the half-space above the surface, that is over the solid angle $\Omega_i = 2\pi$, we obtain the contribution of the scattering to the brightness temperature vector radiated by the rough surface:

$$\begin{aligned} &\mathbf{T}_{\mathbf{B}}^s(\vartheta_s, \varphi_s; 0) \\ &\quad = \frac{1}{4\pi} \int_0^{\pi/2} sin\vartheta_i d\vartheta_i \int_0^{2\pi} d\varphi_i [T_{mDN}[1 - \gamma_{\vartheta_i}(0, \infty)] \\ &\qquad + T_{COS} \gamma_{\vartheta_i}(0, \infty)] \begin{bmatrix} \gamma_{hhhh}(\hat{\mathbf{s}}, \hat{\mathbf{i}}) + \gamma_{h\nu h\nu}(\hat{\mathbf{s}}, \hat{\mathbf{i}}) \\ \gamma_{\nu h\nu h}(\hat{\mathbf{s}}, \hat{\mathbf{i}}) + \gamma_{\nu\nu\nu\nu}(\hat{\mathbf{s}}, \hat{\mathbf{i}}) \\ 2\mathrm{Re}[\gamma_{\nu hhh}(\hat{\mathbf{s}}, \hat{\mathbf{i}}) + \gamma_{\nu\nu h\nu}(\hat{\mathbf{s}}, \hat{\mathbf{i}})] \\ 2\mathrm{Im}[\gamma_{\nu hhh}(\hat{\mathbf{s}}, \hat{\mathbf{i}}) + \gamma_{\nu\nu h\nu}(\hat{\mathbf{s}}, \hat{\mathbf{i}})] \end{bmatrix} \end{aligned} \tag{13}$$

where we have expressed the modified Mueller matrix by using equation (11) and equation (12). Equation (13) relates the vector of brightness temperature of the scattered radiation to the bistatic scattering coefficients. Note that it is not constant with respect to the azimuthal angle and has both U and V components. It is formally very similar to the formula that gives the emitted brightness temperature through the generalized Kirchhoff's law [20]. A relevant difference between the two formulas is due to the presence of $T_B^i = [T_{mDN}(1 - \gamma_{\vartheta_i}(0, \infty)]$, which is function of the incidence angle ϑ_i. This can be understood if we consider that the brightness temperature emitted from the surface is determined by that portion of the radiation coming up from underneath the sea which is transmitted by the sea-air rough interface. The brightness temperature coming up from the sea body is not dependent on the propagating direction and is equal to the physical temperature T_s of the sea, since the dissipative sea water is assumed isothermal and infinite in depth. Therefore, the surface brightness temperature is equal to T_s multiplied by the rough surface transmissivity, that is by one minus the surface reflectivity. Since T_s is constant with the angle, this reflectivity is simply the integral of the bistatic scattering coefficients (considering both the co-polarised and cross-polarised contribution to ensure overall energy conservation). On the contrary, when determining the scattering of the downwelling atmospheric radiation, we have to multiply the bistatic scattering coefficient by the incident brightness temperature, which now is function of the incidence angle.

The apparent brightness temperature vector radiated by a rough surface (at $z = 0$) due to surface emission and scattering is found by adding the emitted brightness temperature vector to equation (13). By using the generalized Kirchhoffs law to express the Stokes emissivity vector $\mathbf{e}(\vartheta_s, \varphi_s)$, it is found:

$$
\begin{aligned}
&\mathbf{T}_{\mathbf{B}}^{ROUGH}(\vartheta_s, \varphi_s; 0) \\
&\quad = \mathbf{T}_{\mathbf{B}}^{e}(\vartheta_s, \varphi_s; 0) + \mathbf{T}_{\mathbf{B}}^{s}(\vartheta_s, \varphi_s; 0) \\
&\quad = T_s \mathbf{e}(\vartheta_s, \varphi_s) + \mathbf{T}_{\mathbf{B}}^{s}(\vartheta_s, \varphi_s; 0) \\
&\quad = T_s \begin{bmatrix} 1 \\ 1 \\ 1 \\ 0 \\ 0 \end{bmatrix} - \frac{1}{4\pi} \int_0^{\pi/2} sin\vartheta_i d\vartheta_i \int_0^{2\pi} d\varphi_i [T_s - T_{mDN} + (T_{mDN}
\end{aligned}
$$

$$- T_{COS})\gamma_{\vartheta_i}(0,\infty)] \begin{bmatrix} \gamma_{hhhh}(\hat{\mathbf{s}},\hat{\mathbf{i}}) + \gamma_{h\nu h\nu}(\hat{\mathbf{s}},\hat{\mathbf{i}}) \\ \gamma_{\nu h\nu h}(\hat{\mathbf{s}},\hat{\mathbf{i}}) + \gamma_{\nu\nu\nu\nu}(\hat{\mathbf{s}},\hat{\mathbf{i}}) \\ 2\mathrm{Re}[\gamma_{\nu hhh}(\hat{\mathbf{s}},\hat{\mathbf{i}}) + \gamma_{\nu\nu h\nu}(\hat{\mathbf{s}},\hat{\mathbf{i}})] \\ 2\mathrm{Im}[\gamma_{\nu hhh}(\hat{\mathbf{s}},\hat{\mathbf{i}}) + \gamma_{\nu\nu h\nu}(\hat{\mathbf{s}},\hat{\mathbf{i}})] \end{bmatrix} \tag{14}$$

When comparing the brightness temperature vector given in equation (14) to the emitted one, it is found that the atmosphere reduces the absolute value of the U and V components due to the azimuth anisotropy of the roughness. The amount of this reduction depends in a complicated way on the angular pattern of the downward atmospheric radiation. The brightness temperature vector observed by the radiometer at altitude H (or at the top of the atmosphere for satellite observations) is then given by equation (10) and the U and V components are further reduced by the factor $\gamma_{\vartheta}(0,H)$.

3. SIMULATION OF ATMOSPHERIC EFFECTS UPON SEA SURFACE POLARIMETRIC SIGNATURE

We have used a software program named SEAWIND that implements the formulation by Yueh [23] which assumes for the sea surface scattering the well known two-scale model [24]. It has been successfully used to compare polarimetric emission of sea to several experimental data sets collected by both ground based and airborne microwave radiometers with polarimetric capability [24]. Due to the similarity of equation (14) to the expression of the emitted brightness temperature, we have implemented only minor changes to the previous version of the software in order to include and quantify the non azimuthally symmetric effect of the atmosphere as theoretically discussed in the previous sections.

In order to introduce realistic values of the two quantities T_m and τ which completely characterize the atmospheric radiative properties in our formulation, we have considered a large number of atmospheric profiles and run radiative transfer models both in non-rainy and rainy conditions. The atmospheric realizations have been provided by radiosoundings, as for non-raining atmosphere and by microphysical models, as for rainy atmosphere. We have run the upgraded SEAWIND software with and without the effect of the atmosphere. The second case is obtained simply by setting the atmosphere transmittance γ and cosmic background T_{COS} to zero, thus obtaining the polarimetric emission of the surface only.

3.1 Electromagnetic Model for Sea Surface Scattering and Emission

Very briefly, the two-scale model assumes that the sea surface is composed of a small wavelength roughness superimposed to large-scale waves. The wave number that separates the two roughness scales is function of the electromagnetic wavelength. From one side it is such that the large waves can be confused with plane patches whose dimensions extend as far as several electromagnetic wavelengths. On the other side, the electromagnetic scattering due to the residual spectrum of small-scale roughness should be interpreted by SPM [12]. Therefore, the brightness temperature vector at the sea surface is due to the incoherent summation of the brightness temperature of each tilted rough patch, provided that the incidence and scattering directions are considered in the reference system joined to the patch. In other words, the brightness temperature vector $\mathbf{T}_\mathbf{B}^{SEA}$ emerging from each patch is averaged over the probability density function $P(S_x, S_y)$ of the slope of the patches, that is over the distribution of slopes S_x and S_y of the large waves:

$$\mathbf{T}_\mathbf{B}^{BOA}(\vartheta_s, \varphi_s; 0) = \int_{-\infty}^{+\infty} dS_y \int_{-\infty}^{+\cot\vartheta} \mathbf{T}_\mathbf{B}^{SEA}(1 - S_x \tan\vartheta) P(S_x, S_y) dS_x \qquad (15)$$

$\mathbf{T}_\mathbf{B}^{SEA}$ is determined by the small scale roughness induced by the wind stress, but it is influenced also by the formation of the foam. For this reason, the brightness temperature vector of the rough surface must be decreased by the fractional foam cover F and increased by the foam unpolarized emission derived by the model proposed by [25]. Besides that, we have also to consider a foam contribution to the scattering of atmospheric radiation. The model by Pandey and Kakar does not give indications about foam bistatic scattering coefficients. For seek of simplicity, we have assumed that the foam scattering is basically specular with an equivalent reflectivity Γ equal to $(1-e_f)$, being e_f the foam emissivity as given by Pandey and Kakar, as assumed by Yueh [23]. Therefore, for a partially foam covered sea the apparent brightness temperature vector emerging from each surface patch is given by:

$$\mathbf{T}_\mathbf{B}^{SEA}(\vartheta_s, \varphi_s; 0) = (1 - F)\mathbf{T}_\mathbf{B}^{ROUGH}(\vartheta_s, \varphi_s; 0) + F e_f T_s \begin{bmatrix} 1 \\ 1 \\ 0 \\ 0 \end{bmatrix}$$

$$+ F(1-e_f)[T_{COS}\gamma_{\vartheta_s}(0,\infty) + T_{mDN}(1-\gamma_{\vartheta_s}(0,\infty)] \begin{bmatrix} 1 \\ 1 \\ 0 \\ 0 \end{bmatrix} \tag{16}$$

where $\mathbf{T}_{\mathbf{B}}^{ROUGH}(\vartheta_s, \varphi_s; 0)$ originates from the wind roughened surface without foam and the transmissivity $\gamma_{\vartheta}(0,\infty)$ is computed at an angle ϑ_i equal to the observation angle ϑ_s. The bistatic scattering coefficients required for computing $\mathbf{T}_{\mathbf{B}}^{ROUGH}$ by equation (14) are given by the second order small perturbation theory, which comprises a coherent ad an incoherent term [12]:

$$\gamma_{\alpha\beta\mu\nu} = R\delta(\vartheta - \vartheta_i; \varphi - \pi_i) + \gamma_{\alpha\beta\mu\nu}^{inc}(\vartheta, \varphi; \vartheta_i, \varphi_i) \tag{17}$$

Given a plane incident wave, the first term represents a plane wave in the specular direction which superimposes the wave reflected according to the Fresnel coefficients in order to ensure overall energy conservation. The second term represents a diffuse radiation and is related to the power density spectrum of the roughness by means of the equations reported in [16].

The bidirectional spectrum of the small scale roughness is derived by Yueh et al. [16] as an adaptation of the Dwrden and Vesecky spectrum, while the bivariate probability density function of the large wave slopes, corresponding to the sea gravity waves, has be assumed Gaussian with different slope variances in the upwind and crosswind directions [23]. Both functions are not isotropic with respect to the azimuth direction and their patterns in azimuth are related to surface wind speed and direction. This is the reason why the scattering coefficients are all different from zero, even those corresponding to the coupling between copolarized incident radiation and cross-polarized scattering (and viceversa) which originate U and V components in the brightness temperature vector. Note that these components are already apparent in equation (14), but they are further modified by the incoherent summation of the patche contributions in a way which is dependent on the large scale slopes. It is worth nothing that even if the ocean wave models are an area of intensive research, they have little impact on the results of our work since we are looking at the differences in the azimuthal signature with and without atmospheric effects.

It should be noted that a further simplification has been implicitly adopted. The atmospheric transmittance $\gamma_\vartheta(0,\infty)$ has been computed for the observing direction in the absolute reference of figure 1, joined to the mean horizontal sea level. In this way we have neglected the multiple scattering, that is we have disregarded the radiation originating by a surface patch that is scattered again by another patch. Alternatively, one could compute $\gamma_\vartheta(0,\infty)$ using the local incidence angle that corresponds to assume that the entire atmosphere is tilting according to the sea large scale slope. Both approaches imply some approximations but, since the slopes of the large scale component of the sea surface are small, the atmospheric transmissivity computed as function of the local incidence angle does not differ significantly from that related to the absolute incidence angle.

3.2 Statistical Evaluation of Atmospheric Emission and Transmission

As far as the non-rainy atmosphere is concerned, we have computed T_m and τ for a large number of atmospheric realizations given by the vertical profiles of temperature, pressure and relative humidity measured by radiosounding balloons launched by the Italian Meteorological Service. In particular, we have used the atmospheric profiles measured along the Tyrrenian coast close to Rome from January 1983 to September 1986. This data set is therefore representative of the atmospheric conditions in the Mediterranean sea environment through the year. We have used a radiative transfer model able to simulate the unpolarized atmospheric brightness temperature measured by a radiometer observing an atmosphere without scattering along a vertical or slanted path. The atmospheric absorption coefficient and the atmospheric refractivity due to the dry and wet (water vapour) components of the atmosphere are computed from the profile of the atmospheric parameters given by radiosoundings. Clear-sky attenuation due to water vapour and oxygen absorption is calculated from the Liebe model [26, 27], which is valid for frequencies up to $1\,\mathrm{THz}$, with oxygen interference coefficients from Rosenkranz [28]. Provided that a number of quality tests on radiosounding data have been passed, the profiles are extrapolated to $0.1\,\mathrm{mbar}$ and interpolated between level when necessary to approximate a continuous atmosphere. The presence of a cloud is detected when the relative humidity exceeds a certain level (which has been assumed equal to 95%). The base and the top of the cloud

and the cloud density are evaluated by the model of Decker et al. [29].

The equivalence of a plane-parallel atmosphere to an homogeneous layer represented by equations (7) and (8) is exactly true only in the absence of scattering. However, in order to be able to apply equation (14), we have used the same formula even in the presence of light precipitating clouds. To this aim, we have computed the brightness temperature T_{UP} and T_{DN} for a plane-parallel atmosphere in the presence of precipitating clouds by using a radiative transfer algorithm that solves for the scattering contribution by means of the discrete ordinate method as explained in [18]. It assumes all scattering particles (hydrometeors) are spherical with single scattering properties derived by Mie theory and averaged on the statistical distribution of particle size. Then, we have evaluated the parameters of an equivalent homogeneous atmosphere. The atmospheric transmittance was computed by integrating along a vertical or a slanted path the extinction coefficient k_e, while the mean radiative temperatures have been derived from the brightness temperature given by the model using equations (7) and (8). In this computation we have imposed the boundary condition at the Earth surface by assigning the physical temperature and a surface emissivity different for vertical and horizontal polarizations and derived from the outputs of the polarimetric emission model (note that in this case the interaction between the surface and the atmosphere influences T_{UP} also). It must be pointed out that in this case equations (7) and (8) do not give the precise behavior of T_{DN} and T_{UP} as function of angle ϑ. However, since only light precipitations are interesting for radiometric applications over sea, the relation may be considered accurate enough.

A fairly realistic precipitating cloud data base has been provided by Pierdicca et al. [18]. The data base contains a large number of cloud structures belonging to five different cloud typologies (classes). Each cloud consists of seven homogeneous layers and is completely identified by the density of four hydrometer species (rain, ice, precipitable rain and graupel) in each layer, plus the dielectric properties and the size distribution of these hydrometeors and the profiles of temperature, pressure and water vapour. The hydrometeor contents in each layer have been generated statistically as realizations of a multivariate Gaussian random variable, whose covariance matrix has been derived, for each class, by statistically analyzing the output of a microphysical model simulating the time evolution of a convective storm [30]. In this way, the data base preserves the original correlation between

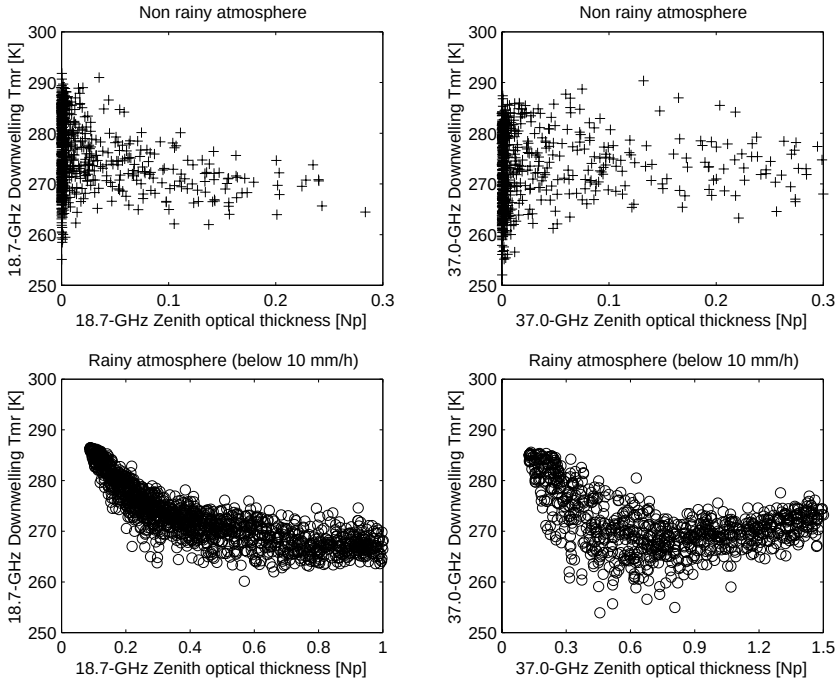

Figure 2. Downwelling mean radiative temperature T_{mDN} (in K) at 50° off-zenith angle versus zenithal optical thickness τ due to atmospheric gases and non-rainy clouds (top panels) and to precipitating clouds with rain below 10 mm/h (bottom panels) at 18.7 GHz (left panels) and at 37.0 GHz (right panels). Data points are derived by applying a radiative transfer model to 4-year radiousounding data (Rome, 1983–86) and to simulated precipitating clouds, respectively.

hydrometeor contents at different altitude levels due to the microphysical constraints contained in the cloud model. We have considered only a subset of the cloud data base that corresponds to classes of clouds with moderate scattering particle contents. In particular, a maximum rain intensity of 10 mm/hr has been considered, which corresponds in the data base to a maximum equivalent water content of all precipitating hydrometeors of about $1.5\,\mathrm{kg/m^2}$.

The values of τ, T_{mDN} and T_{mUP} have been computed at the frequency channels potentially relevant for sea applications (i.e., 18.7 and 37 GHz). The scatterplots of T_{mDN} as function of τ are presented in Figure 2, where the values derived from radiosoundings and those

	10 GHz	18.7 GHz	22.2 GHz	37 GHz
τ	0.014	0.047	0.141	0.082
T_{mDN}	269	276	277	272

Table 1. Median values of atmospheric opacities τ (in neper) and mean radiative temperatures T_{mDN} and T_{mUP} (in K) derived from radiosoundings (Rome, January '83 to September '86) for scattering-free atmosphere.

derived from the precipitating cloud database are shown separately, the latter being limited to rain rates below 10 mm/hr. It can be observed that the opacity of a non-precipitating atomosphere is weekly correlated to the mean radioative temperature. When the opacity increases due to higher liquid water content the T_m tends to decrease since the emission originating from the higher and colder atomosphere layer prevails. The scattering by particles of a precipitating cloud obviously increases the opacity and extinguishes the atmosphere radiation, thus making T_m generally decrease. Table 1 reports the median values of these quantities for non-precipitation conditions. As for precipitating conditions, the median values of T_{mDN} changes very little (274 K at 18.7 GHz and 277 K at 37 GHz) while the opacity at zenith may exceed 1 neper at the higher frequency (0.377 neper at 18.7 GHz and 1.19 neper at 37 GHz).

3.3 Analysis of Model Results

In this section we present some examples of the polarized radiation measured above the sea surface both including and not including the contribution from the atmosphere. The computations have been performed at 18.7 GHz and 37 GHz by using the typical values of τ, T_{mDN} and T_{mUP} found in the previous section.

In Figure 3 the upper panels show the first two elements (T_{Bh} and T_{Bv}) of the brightness temperature vector $\mathbf{T_B}$ at 18.7 GHz, while the bottom panels present the last two elements (U and V), in both cases as function of the azimuth angle φ between radiometer observation and wind directions. The figure shows the emitted $\mathbf{T}^e_{\mathbf{B}}(\vartheta, \varphi; 0)$ vector in the absence of atmosphere, the $\mathbf{T}^{BOA}_{\mathbf{B}}(\vartheta, \varphi; 0)$ vector radiated by the surface and including emission and scattering as in equations

(15) and the $\mathbf{T_B}^{TOA}(\vartheta, \varphi; 0)$ vector given by equation (10) observed by a spaceborne radiometer at the top of the atmosphere. The wind speed is $10.6\,\mathrm{m/s}$ and the atmosphere is characterized by $\tau = 0.047$ and $T_{mDN} = 276\,\mathrm{K}$, that is values that are exceeded 50% of the time, according to the radiosounding data base. Values of comparable magnitude have been found also by Yueh et al. when attempting to correct for the atmospheric effect in radiopolarimetry [31]. It is apparent the effect of the small scale roughness anisotropy that causes a non zero value for the U and V components and a periodic dependence with respect to wind direction with period π. A further periodic component of period 2π in the U and V signals is due to the hydrodinamical modulation of the small waves above the large waves taken into account in the adopted small scale sea surface spectrum. This effect, and specifically the presence of U and V components in the measured brightness temperature vector, may allow one to estimate wind direction from measurements of a polarimetric radiometer. The interesting fact that is addressed by the figure is the effect of the atmospheric scattering which slightly decreases the U and V harmonic components observed at the bottom of the atmosphere. The more obvious effect of the atmospheric attenuation of such components when observing at the top of the atmosphere is also quantified in the figure. The reduction of the T_{Bh} and $T_{B\nu}$ harmonic components is also present, even though it is not evident in the figure.

Figure 4 shows the same quantities at $37\,\mathrm{GHz}$ computed by assuming again the atmospheric parameters given in Table 1. Once again, the maximum and minimum values in the U and V signals are influenced by the presence of the atmosphere at an extent which now is not negligible when compared to the small values of these quantities (particularly V). Since the U and V signals are in the order of $1\,\mathrm{K}$ or less, it is evident that a typical atmosphere at middle latitude and marine environment may decrease such signal by about 10%.

A part from the obvious conclusion that the atmosphere influences the measured brightness temperature, what is more interesting in this simulation is the quantification of the atmospheric contribution to the variations of $\mathbf{T_B}$ harmonic components with respect to φ. This influence can be expressed only in terms of atmospheric attenuation as done in [31] or in the approximated model in [32]. However, we have verified that it is also function of the wind speed and this has to be properly taken into account in the model function to be considered for

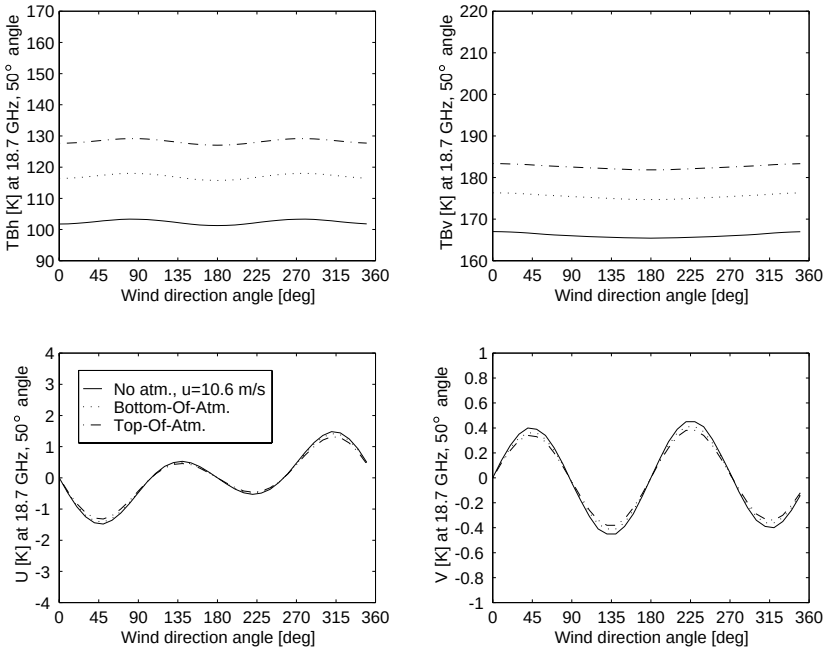

Figure 3. Stokes-vector components of upwelling brightness temperature T_B (T_{Bh}, T_{Bv}, U, and V) at 18.7 GHz and 50° off-nadir angle, as a function of the wind direction angle, supposing a near-surface wind velocity of 10.6 m/s. Results at Bottom-Of-the-Atmosphere (T_B^{BOA}) include only the downwelling atmospheric brightness temperature contribution, while those at the Top-Of-the-Atmosphere (T_B^{TOA}) include both the downwelling and upwelling atmospheric brightness temperature effects. For comparison, the Stokes vector behavior without any atmospheric effect is also plotted.

polarimetric radiometers. Moreover, attention should be paid to this problem when specifying requirements of the radiometric instrumentation and setting up the procedure to retrieve wind direction.

4. A MODEL FUNCTION FOR CORRECTING ATMOSPHERIC EFFECTS IN RADIOPOLARIMETRY OF THE SEA

The radiation emitted by the rough sea surface, given the observation angle and the frequency band, can be expressed as function of the wind

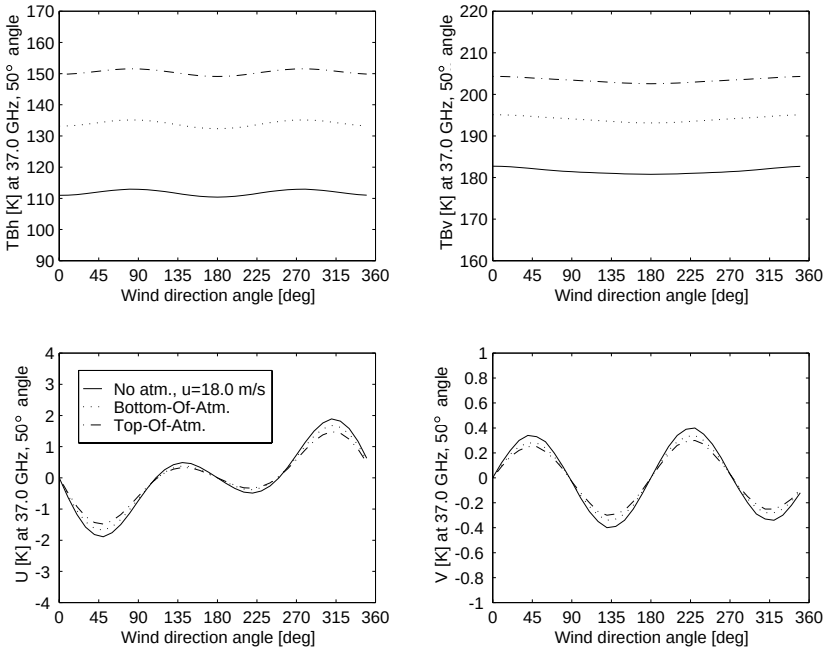

Figure 4. Same as in Figure 2, but at 37.0 GHz and 18 m/s wind speed.

direction and wind speed, provided that sea salinity and temperature can be assumed constant. As far as wind direction is concerned, the components of the emitted brightness temperature vector can be expressed throughout a combination of two harmonics of period 2π and π respectively, or equivalently as the combination of $\cos\varphi$ and $\cos^2\varphi$:

$$\begin{aligned} I_h^e &= I_h^{e(0)} + I_h^{e(1)}\cos\varphi + I_h^{e(2)}\cos 2\varphi \\ &= B_h^{e(0)} + B_h^{e(1)}\cos\varphi + B_h^{e(2)}\cos^2\varphi \\ I_\nu^e &= I_\nu^{e(0)} + I_\nu^{e(1)}\cos\varphi + I_\nu^{e(2)}\cos 2\varphi \\ &= B_\nu^{e(0)} + B_\nu^{e(1)}\cos\varphi + B_\nu^{e(2)}\cos^2\varphi \\ U^e &= U^{e(1)}\sin\varphi + U^{e(2)}\sin 2\varphi = B_U^{e(1)}\cos\varphi + B_U^{e(2)}\cos^2\varphi \\ V^e &= V^{e(1)}\sin\varphi + V^{e(2)}\sin 2\varphi = B_V^{e(1)}\cos\varphi + B_V^{e(2)}\cos^2\varphi \end{aligned} \tag{18}$$

The dependence of each harmonic with wind speed may be determined by a regression model trained by the output of the simulation program

as done in [31].

The effect of the atmosphere can be considered by introducing the quantities $\tau(0,\infty)$, T_{mDN} and T_{mUP}. While the vertical atmospheric opacity $\tau(0,\infty)$ must be considered unknown, the downwelling mean radiative temperature T_{mDN} can be determined with good accuracy (within a few degrees) as function of the sea surface temperature measured by remote sensors or derived by climatology [3]; the same applies to T_{mUP} that is just a few degree below T_{mDN}. The total radiation at the sea surface (both emitted and scattered) is given by equations (11), (15) and (16) where, as already mentioned, the scattering contribution has a very complicated expression. In case the radiometer operates within an atmospheric window and in the absence or for very light precipitation, the atmospheric opacity is less than one. Therefore, we can assume an approximate expression for the slanted transmittance, that is based on the Taylor approximation with respect to the transmittance of a vertical path $\gamma(0,\infty) = \exp[-\tau(0,\infty)]$, with starting point $\gamma(0,\infty) = 1$:

$$\begin{aligned} T_{mDN} - (T_{mDN} - T_{COS})\gamma_\vartheta(0,\infty) \\ \approx T_{COS} + (T_{mDN} - T_{COS})[1 - \gamma(0,\infty)]\sec\vartheta \end{aligned} \tag{19}$$

By disregarding T_{COS} to simplify the notation and substituting equation (19) in equation (13), the atmospheric parameters go out of the integrals. Therefore, it is possible to assume even for $\mathbf{T}^s_{\mathbf{B}}$ a model function which is simply linearly related to the atmospheric radiative parameters T_{mDN} and $\gamma(0,\infty)$ and contains two harmonics as for the dependence on φ:

$$\begin{aligned} I^s_h &= (T_{mDN} - T_{COS})[1 - \gamma(0,\infty)][B^{s(0)}_h + B^{s(1)}_h \cos\varphi + B^{s(2)}_h \cos^2\varphi] \\ I^s_\nu &= (T_{mDN} - T_{COS})[1 - \gamma(0,\infty)][B^{s(0)}_\nu + B^{s(1)}_\nu \cos\varphi + B^{s(2)}_\nu \cos^2\varphi] \\ U^s &= (T_{mDN} - T_{COS})[1 - \gamma(0,\infty)][B^{s(1)}_U + B^{s(2)}_U \sin\varphi\cos\varphi] \\ V^s &= (T_{mDN} - T_{COS})[1 - \gamma(0,\infty)][B^{s(1)}_V + B^{s(2)}_V \sin\varphi\cos\varphi] \end{aligned} \tag{20}$$

The coefficients $B^{s(i)}_h$, $B^{s(i)}_\nu$, $B^{s(i)}_U$, and $B^{s(i)}_V$ multiplied by $(T_{mDN} - T_{COS})[1 - \gamma(0,\infty)]$ quantify the reduction of the harmonic coefficients in equation (18) due to the atmosphere radiation scattering. They have been derived by fitting the SEAWIND software output as function of the wind speed W (in m $\sec^{-1}$). If we indicate with $B^{(i)}$ any of the

		$B^{(0)}$			$B^{(1)}$		$B^{(2)}$	
		b_{00}	$b_{01}\,10^3$	$b_{02}\,10^3$	$b_{11}\,10^3$	$b_{13}\,10^6$	$b_{21}\,10^3$	$b_{23}\,10^6$
18.0 GHz	I_h	1.228	-2.415	-0.284	0.516	0.137	-0.978	0.718
	I_ν	0.765	0.187	-0.116	0.233	0.102	-1.312	0.856
	U	/	/	/	$.35\ \ 10^{-6}$	0.0	0.706	-0.297
	V	/	/	/	$.14\ \ 10^{-6}$	0.0	-0.541	-0.226
37.0 GHz	I_h	1.036	8.166	-0.666	0.521	0.562	-0.595	0.530
	I_ν	0.573	5.557	-0.295	0.0964	0.0323	-1.533	0.642
	U	/	/	/	0.228	0.493	1.369	-0.279
	V	/	/	/	0.0138	0.050	-0.420	-0.511

Table 2. Zero-, first- and second-order harmonics ($B^{(0)}$, $B^{(1)}$ and $B^{(2)}$, respectively) of equation (20) to model the contribution to $\mathbf{T}_\mathbf{B}^{BOA}$ of scattering of atmospheric radiation. The harmonics are given as function of wind speed W (m/s) as given in equation (20). The coefficients of polynomial regression (20) that are negligible have been omitted.

considered coefficients with i ranging from 0 to 2, we have assumed the following dependence on wind speed:

$$\begin{aligned} B^{(0)} &= b_{00} + b_{01}W + b_{02}W^2 + b_{03}W^3 \\ B^{(1)} &= b_{10} + b_{11}W + b_{12}W^2 + b_{13}W^3 \\ B^{(2)} &= b_{20} + b_{21}W + b_{22}W^2 + b_{23}W^3 \end{aligned} \tag{21}$$

The coefficients of the regression we have found are shown in Table 2. They can be used for quantifying the scattering of the atmospheric radiation in the model function (18) used to retrieve the unknown wind speed from the polarimetric measurements. It is required to know T_m and τ in some way, such as using radiosoundings, meteorological surface data or multifrequency radiometers.

5. CONCLUSIONS

In this work the scattering of the downward atmospheric radiation by an azimutally anisotropic rough surface has been analyzed. It has been demonstrated that, even for unpolarized atmospheric emission, the scattered radiation is partially polarized. Therefore, the U and

V component in the brightness temperature vector emitted by an azimutally anisotropic rough surface are modified in the presence of the atmosphere. This modification may influence the possibility of retrieving the wind speed over the sea surface from passive measurements of the polarization state which has been indicated by several authors. Using a software package which simulates the sea surface roughness by the two-scale model and accounts for the presence of foam, the effect of the atmosphere on the polarimetric passive microwave signature has been quantified, paying particular attention to the U and V components. Using a data base of realistic atmospheric structures derived from radiosounding and cloud models, it has been shown that the U and V components may be decreased of 10% in standard atmospheric conditions at $37\,\mathrm{GHz}$. A model function has been proposed to account for this effect as function of the wind direction by introducing two harmonics with period π and 2π. The unknown quantities in this model function are the atmospheric opacity and, partially, the mean radiative temperature. The dependence of the harmonic amplitudes with wind intensity has been assumed quadratic and regression coefficients have been determined from the output of the simulation package. This model function can be helpful to correct the experimental data and two specify system requirements for a polarimetric radiometer able to measure wind speed and direction over sea.

ACKNOWLEDGMENT

We are grateful to the Italian Meteorological Service for providing the radiosounding data and to Prof. J. A. Kong for his helpful contribution to the development of the SEAWIND software. The work has been funded by the European Space Agency under contract No. 1146/95/NL /NB.

REFERENCES

1. Phillips, O. M., *The Dynamics of the Upper Ocean,* Cambridge University Press, New York, 1977.
2. Ulaby, F. T., R. K. Moore, and A. K. Fung, *Microwave Remote Sensing. Active and Passive,* Addison-Wesley, Reading, MA, 1981.
3. Wentz, F. J., L. A. Mattox, and S. Peteherych, "New algorithms for microwave measurements of ocean winds: applications

to SEASAT and the special sensor microwave imager," *J. Geophys. Res.,* Vol. 19(C2), 2289–2307, 1986.

4. Goodberlet, M. A., C. A. Swift, and J. C. Wilkerson, "Ocean surface wind speed measurements of the special sensor microwave imager (SSM/I)," *IEEE Trans. Geosci. and Rem. Sens.,* Vol. 28, No. 5, 823–828, 1990.
5. Moore, R. K., A. H. Chaudry, and I. J. Birrer, "Errors in scatterometer-radiometer wind measurement due to rain," *IEEE J. Oceanic Eng.,* Vol. 8, 37–49, 1983.
6. Sobieskii, P., A. Guissard, and C. Baufays, "Synergic inversion techniques for active and passive microwave remote sensing of the ocean," *IEEE Trans. Geosci. and Rem. Sens.,* Vol. 29, No. 3, 391–406, 1993.
7. Wentz, F. J., "Measurement of oceanic wind vector using satellite microwave radiometers," *IEEE Trans. Geosci. and Rem. Sens.,* Vol. 30, No. 5, 960–972, 1992.
8. Dzura, M. S., V. S. Etkin, A. S. Khrupin, M. N. Pospelov, and M. D. Raev, "Radiometers-polarimeters: principles of design and applications for sea surface microwave emission polarimetry," *Proc. IGARSS'94, IEEE N.94CH3378-7,* 1432–1434, 1994.
9. Gasiewski, A. J., and D. B. Kunkee, "Polarized microwave emission from water waves," *Radio Science,* Vol. 29, No. 6, 1449–1466, 1994.
10. Yueh, S. H., W. J. Wilson, F. K. Li, S. V. Nghiem, and W. B. Ricketts, "Polarimetric measurements of sea surface brightness temperatures using an aircraft K-band radiometer," *IEEE Trans. Geosci. and Rem. Sens.,* Vol. 33, No. 1, 85–92, 1995.
11. Veysoglu, M. E., H. A. Yueh, R. T. Shin, and J. A. Kong, "Polarimetric passive remote sensing of periodic surfaces," *J. Electrom. Waves Applic.,* Vol. 5, No. 3, 267–280, 1991.
12. Yueh, H. A., R. T. Shin, and J. A. Kong, "Scattering of electromagnetic waves from a periodic surface with random roughness," *J. Appl. Phys.,* Vol. 64, No. 4, 1657–1670, 1988.
13. Johnson, J. T., J. A. Kong, R. T. Shin, D. H. Staelin, K. O'Neill, and A. Lohanick, "Third stokes parameter emission from a periodic water surface," *IEEE Trans. Geosci. and Rem. Sens.,* Vol. 31, No. 5, 1066–1080, 1993.
14. Yueh, S. H., S. V. Nghiem, W. Wilson, F. K. Li, J. T. Johnson, and J. A. Kong, "Polarimetric thermal emission from periodic water surface," *Radio Science,* Vol. 29, No. 1, 87–96, 1994.
15. Johnson, J. T., J. A. Kong, R. T. Shin, S. H. Yueh, S. V. Nghiem, and R. Kwok, "Polarimetric thermal emission from rough ocean surfaces," *J. Electrom. Waves Applic.,* Vol. 8, No. 1, 43–59, 1994.

16. Yueh, S. H., R. Kwok, F. K. Li, S. V. Nghiem, W. J. Wilson, and J. A. Kong, "Polarimetric passive remote sensing of ocean wind vectors," *Radio Science,* Vol. 29, No. 4, 799–814, 1994.
17. Swift, C. T., and L. Hevisi, "Design of a Ka band polarimetric radiometer," *Proc. IGARSS'94, IEEE N.94CH3378-7,* 2419–2420, 1994.
18. Pierdicca, N., F. S. Marzano, G. d'Auria, P. Basili, P. Ciotti, and A. Mugnai, "Precipitation retrieval from spaceborne microwave radiometers using maximum a posteriori probability estimation," *IEEE Trans. Geosci. and Rem. Sens.,* Vol. 34, 831–846, 1996.
19. Pospelov, M. N., "Surface wind speed retrieval using passive microwave polarimetry: the dependence on atmospheric stability," *IEEE Trans. Geosci. and Rem. Sens.,* Vol. 34, 1166–1171, 1996.
20. Yueh, S. H., and R. Kwok, "Electromagnetic fluctuations for anisotropic media and the generalized Kirchhoff's law," *Radio Science,* 28, 471–480, 1993.
21. Ulaby, F. T., and C. Elachi, *Radar Polarimetry for Geoscience Applications,* Artech House, Norwood, 1992.
22. Tsang, L., J. A. Kong, and R. Shin, *Theory of Microwave Remote Sensing,* A Wiley Interscience publication, John Wiley & Sons, Inc., New York, 1985.
23. Yueh, S. H., "Modeling of wind direction signals in polarimetric sea surface brightness temperatures," *IEEE Trans. Geosci. and Rem. Sens.,* Vol. 35, 1400–1418, 1997.
24. Pampaloni, P., L. Guerriero, G. Macelloni, and N. Pierdicca, "'SEAWIND': a physical model for simulating ocean wind measurements by means of radio polarimetry," *Proc. of an International Workshop POLRAD 96 Polarimetric Radiation,* ESA WPP-135, ISSN 1022-6656, August 1996.
25. Pandey, P. C., and R. K. Kakar, "An empirical microwave emissivity model for a foam-covered sea," *IEEE Journal of Oceanic Engineering,* 7, 3, 165–140, 1982.
26. Liebe, H. J., "An updated model for millimeter propagation in moist air," *Radio Sci.,* 20, 1069–1089, 1985.
27. Liebe, H. J., "An updated model for millimeter propagation in moist air," *Radio Sci.,* Vol. 20, 1069–1089, 1995.
28. Rosenkranz, P. W., "Interference coefficients for overlapping oxygen lines in air," *J. Quant. Spectrosc. Radiat. Transfer,* 39, 87–97, 1988.
29. Decker, M. T., E. R. Westwater, and F. O. Guiraud, "Experimental evaluation of ground-based microwave radiometric remote sensing of atmospheric temperature and water vapour profiles," *J. Applied Meteorology,* 17, 1788–1795, 1978.

30. Smith, E. A., A. Mugnai, H. J. Cooper, G. J. Tripoli, and X. Xiang, "Foundations for statistical- physical precipitation retrieval from passive microwave satellite measurements. Part I: Brightness-temperature properties of a time-dependent cloud-radiation model," *J. Appl. Meteor.,* 31, 6, 506–531, 1992.
31. Yueh, S. H., W. J. Wilson, S. J. Dinardo, and F. K. Li, "Polarimetric microwave brightness signature of ocean wind directions," *IEEE Trans. Geosci. and Rem. Sens.,* Vol. 37, 949-959, 1999.
32. Yeong, C. P., S. H. Yueh, K. H. Ding, and J. A. Kong, "Atmospheric effect on microwave polarimetric passive remote sensing of ocean surfaces," *Radio Science,* 34, 2, 521–537, 1999.